

Received January 29, 2019, accepted February 24, 2019, date of publication March 1, 2019, date of current version March 18, 2019.

Digital Object Identifier 10.1109/ACCESS.2019.2901964

# LTE MIMO Closed Slot Antenna System for Laptops With a Metal Cover

SHU-CHUAN CHEN<sup>1</sup>, (Member, IEEE), AND MING-CHAN HSU<sup>2</sup>

<sup>1</sup>Electrical and Electronic Engineering Department, Chung Cheng Institute of Technology, National Defense University, Taoyuan 335, Taiwan

<sup>2</sup>Department of Electrical Engineering, National Yunlin University of Science and Technology, Yunlin 640, Taiwan

Corresponding author: Shu-Chuan Chen (scchen0319@gmail.com)

This work was supported by the Ministry of Science and Technology, Taiwan, under Grant MOST 107-2221-E-606-004-.

**ABSTRACT** This paper presents an LTE MIMO closed slot antenna system for laptops with a metal cover. Its main and auxiliary antennas have the same structure that measures  $130 \times 3 \text{ mm}^2$ . They are configured in a manner of reflection symmetry on the display metallic ground plane and are 5 mm away from the hinge. The distance between the two antennas is 20 mm, and the profile height of the MIMO antenna system is only 3 mm. This LTE closed slot antenna is excited by an exciter of  $30 \times 3 \text{ mm}^2$  to cover the LTE eight-band operation (LTE700/GSM850/900/1800/1900/UMTS/LTE2300/2500). The exciter is a simple planar inverted-F antenna (PIFA) structure loaded with reactive matching elements, which can enhance the impedance matching in the desired frequency bands. This LTE MIMO closed slot antenna system has good isolation of at least 16 dB without adding any additional isolation elements. The measured antenna efficiency of the MIMO antenna system is larger than 40% in the low-frequency band and 50% in the high-frequency band, meeting the practical application requirements.

**INDEX TERMS** Laptop antennas, closed slot antennas, LTE MIMO antennas, ECC (envelope correlation coefficient).

## I. INTRODUCTION

With the popularity of the fourth-generation (4G) mobile communication long-term evolution (LTE) technology and the demand for fast wireless transmission rates, multiple-input multiple-output (MIMO) systems have been widely used in many mobile communication devices to respond to today's massive data transmission. In addition, thin portable smart phones, tablets, or laptops with a fashionable appearance of a metal cover and a high screen-to-body ratio are a trend-setting mobile communication device. However, the large screen-to-body ratio, metal back cover, and slim appearance restrict the space allowed for antenna design. On the basis of the above conditions, it is a serious challenge for antenna researchers to configure in an internal-space-limited metal-cover mobile communication device an LTE MIMO antenna system with high isolation.

High transmission speed, light weight, thin appearance, and fashionable metal texture of the cover are the features that most consumers require nowadays when choosing mobile

communications products. Therefore, the antenna features of miniaturization, low profile, easy integration with the mobile device's metal frame, and multiband operation have been the goals that antenna designers are pursuing. Among the antennas revealed in recent years [1]–[12], the required operating bandwidth has been covered mainly by adding multiple segments of metal branches [1], [2] or by exciting the resonant modes of the slot structure [3], [4]. Moreover, matching circuits formed by chip capacitors and inductors have been used to enhance the antenna bandwidth and reduce the antenna size [5]–[8]. Other antennas have integrated metal covers or metal frames as part of the radiation structure [9]–[14], including using a slot structure with high-pass and low-pass matching circuits to increase the bandwidth [9]–[12], using integrated metal frames to form a loop structure [13], and using integrated metal frames and metal ground planes to form a slot structure [14]. With surrounding metals closely integrated, all the structures adopted in [9]–[14] can effectively miniaturize the antenna and reduce the antenna's profile height. In the above-mentioned antennas that can support LTE eight-band operation, the minimum antenna profile height required is still as large as 7 mm [9]–[12]. This large profile height

The associate editor coordinating the review of this manuscript and approving it for publication was Mohammad Tariqul Islam.

severely limits the screen-to-body ratio that can be achieved in a mobile communication device. Hence, for the purpose of maximizing that ratio, it is worth our effort to further reduce the antenna's profile height. Moreover, the desired ratios of the high modal frequencies to the low ones in [11] and [12] were achieved by implementing meandered slots, which in terms of aesthetic perception are less preferred than simple straight slots.

**TABLE 1. Comparison of the LTE MIMO antenna system for laptop computer applications.**

Ref.	antenna size width × length	Strengths	Weaknesses
17	16 mm × 29 mm	good isolation	1. Large antenna size. 2. Isolation components are needed
18	2 mm × 60 mm	1. Simple antenna structure with low profile 2. Good isolation	1. Isolation component is needed. 2. Isolation component size is larger than antenna's.
19	4 mm × 84 mm	1. Simple antenna structure 2. Good isolation without isolation component	1. Antenna performance may be downgraded by the opening and closing. 2. Only suitable for specific styles.
20	5 mm × 25 mm	1. Simple antenna structure with low profile 2. Good isolation	1. Antenna performance may be downgraded by the opening and closing. 2. Only suitable for specific styles.
proposed	3 mm × 130 mm	1. Simple antenna structure with low profile 2. Good isolation without isolation component	Only suitable for specific styles.

In order to satisfy consumers' demand for narrow-bezel (or narrow-edge-frame) and metal-textured mobile communication devices, some recently introduced antennas have been configured in the hinge slot region of a laptop computer so that the laptop computer can have a large screen with a full metal cover [15], [16]. Currently, in the design of an LTE MIMO antenna system for laptop computers (refer to Table 1 for comparison), a resonator in LTE700 and LTE2300/2500 band is used to reduce the mutual coupling between two adjacent antennas [17], and a T-type isolation element is used to trap the ground-plane surface current between the main and auxiliary antennas so that the mutual coupling can be reduced [18]. Unfortunately, the isolation elements adopted in the above two cases occupy too much space since their sizes are about the same as those of the antennas themselves, and hence further improvement should be carried out. In addition, there is also research for the MIMO antenna system configured between the hinges [19], [20]. This type of design is beneficial to the realization of an all-metal cover and

can produce multiple frequency bands. In [19], the MIMO antenna system is designed by connecting the metal hinges, ground planes, and numerous properly configured metal connectors to form several open and closed slots. Such a design can only be realized with specific coordination of the mechanism's appearance, and thus is limited in practical application. In [20], the MIMO antenna system is configured in the closed hinge-slot region of the laptop, and a metal sheet is placed between the two antennas to optimize the isolation. Because the system uses the exciter to excite the hinge-slot modes, the antenna performance may be downgraded by the coupling variation owing to multiple times of opening and closing the laptop.

To solve the above issues, this paper proposes an LTE MIMO closed slot antenna system that is configured on the display ground plane and that can produce all LTE bands. The salient features of this design are that only straight slots are needed, the profile height of the antenna can reach a record low of only 3 mm, and a high screen-to-body ratio can be achieved. This closed slot antenna with 3 mm profile height covering all LTE bands is the lowest-profile LTE antenna structure design [9]–[12], [18]–[20]. In addition, no isolation element is needed in the proposed design that is very suitable for laptops with a metal cover.

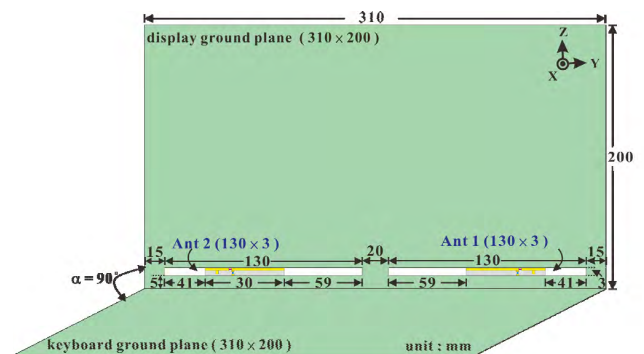


**FIGURE 1. Overall configuration of the proposed LTE MIMO antenna system.**

## II. PROPOSED MIMO ANTENNA SYSTEM DESIGN

### A. MIMO ANTENNA SYSTEM STRUCTURE

Figure 1 shows the overall configuration of the proposed LTE MIMO antenna system. As shown in the figure, the display ground plane and keyboard ground plane of this design are both 310 × 200 mm<sup>2</sup> in dimension. Such a dimension is commonly seen in 14-inch laptops available on the market. It is noteworthy that no conventional elongated hinge slot exists between two ground planes, such as Surface Book 2, Yoga 3 Pro and YOGA C930, etc. The LTE MIMO antenna system consists of two closed-slot antennas of the same size and structure, with each slot measuring 130 mm in length and 3 mm in width. The main and auxiliary antennas are configured on the display ground plane with reflection symmetry. With a short distance of only 20 mm in between, they are placed 5 mm away from the hinge, and 15 mm away

from the two sides of the display ground plane. Although no additional isolation element is included in the design, a measured in-band isolation of larger 16 dB can be achieved, as will be shown later. Here, the main and auxiliary antennas are denoted by Ant 1 and Ant 2, respectively.

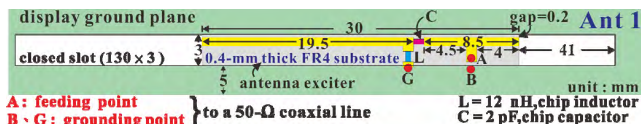


FIGURE 2. Structural details of Ant 1.

Because Ant 1 and Ant 2 have the same structure, only the design mechanism of Ant 1 is explained here. Figure 2 shows the detailed structure of Ant 1, which is a closed slot of  $130 \times 3 \text{ mm}^2$  with an exciter inside. The exciter is designed to excite the resonant modes of the closed slot to produce the required LTE frequency bands. This exciter is printed on an FR4 substrate with a thickness of 0.4 mm and a size of  $30 \times 3 \text{ mm}^2$ . The FR4 substrate, 41 mm away from the right-end of the slot, has a relative dielectric constant of 4.4 and a loss tangent of 0.02. This exciter is a planar inverted-F antenna (PIFA) loaded with LC matching elements that can effectively increase the matching bandwidth at low and high bands. Point A in the figure is the feeding point of the exciter, which is connected to the inner conductor of a 50-Ω mini coaxial line, while Point B is the grounding point linked to the outer conductor of the coaxial cable, and point G is the grounding point of the shorting segment. For impedance-matching enhancement, a surface-mount chip inductor ( $L = 2 \text{ nH}$ ) is inserted into the shorting segment, and a surface-mount chip capacitor ( $C = 2 \text{ pF}$ ) is inserted into the horizontal metal segment just to the right of the shorting segment. The inserted chip inductor can enhance the impedance matching in both the low- and high-frequency bands, whereas the inserted chip capacitor can increase the operating bandwidth of the low-frequency band, so that the eight LTE bands can be covered the detailed design mechanism will be explained later.

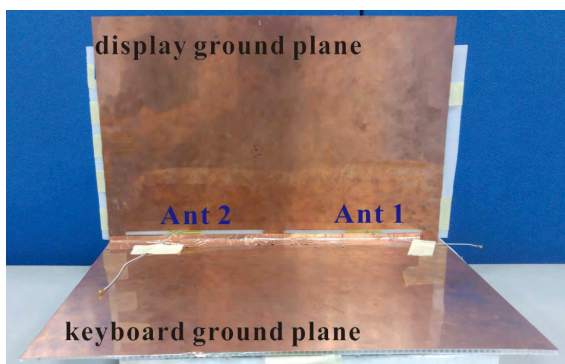


FIGURE 3. Photographs of the proposed MIMO antenna system.

**B. EXPERIMENT AND MEASUREMENT RESULTS**

Figures 3 and 4 show the photographs of the proposed MIMO antenna system and Ant 1, respectively. Figure 5 shows



FIGURE 4. Photograph of Ant 1.

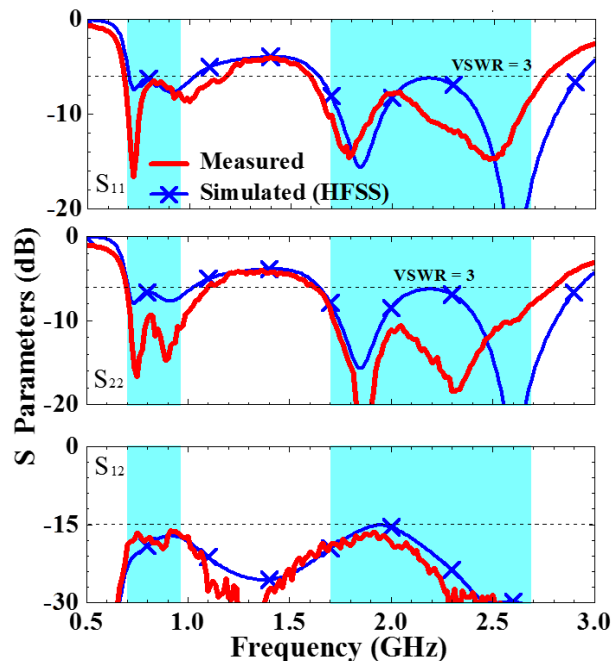


FIGURE 5. Simulated and measured S-parameters of the proposed LTE MIMO antenna system.

the reasonably agreed measured and simulated S-parameters of the proposed MIMO antenna system. For either simulated or measured data, the impedance bands cover three low bands (LTE700/GSM850/900) and five high bands (GSM1800/1900/UMTS/LTE2300/2500). Here, the adopted criterion for the impedance bands is the 6 dB return loss (or, equivalently, the 3:1 standing-wave ratio), which is widely applied to current mobile communications devices. This LTE MIMO closed slot antenna system has a good measured isolation ( $|S_{12}|$ ) performance of at least 16 dB without implementing any additional isolation element. The simulation software used in this research was ANSYS HFSS® (Version 15) [21]. It can be seen that there are some deviations between the measured and simulated return loss, which may be caused by the introduced coaxial cable in the experiment and the discrepancies in the simulated and fabricated parameters of the FR4 substrate.

The above LTE eight-band operating frequencies are generated by four resonant modes contributed by closed slot: Modes 1, 2, 3, and 4. For convenience, these modes are associated with the dip frequencies of the reflection-coefficient curves in figure 5. In the ascending sequence observed from the simulated reflection coefficients for Ant 1, they occur at 710 MHz (Mode 1), 910 MHz (Mode 2), 1840 MHz (Mode 3), and 2600 MHz (Mode 4). Figure 6 demonstrates

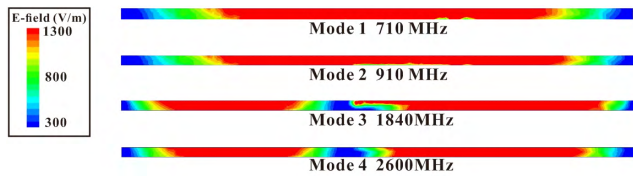


FIGURE 6. Simulated electric field distributions in the closed slot hosting Ant 1 at 710, 910, 1840, 2600 MHz.

the simulated electric field distributions in the closed slot for Ant 1 at these four frequencies. Obviously, the first two modes are in half-wavelength resonance in the closed slot, and the remaining two modes in full-wavelength resonance.

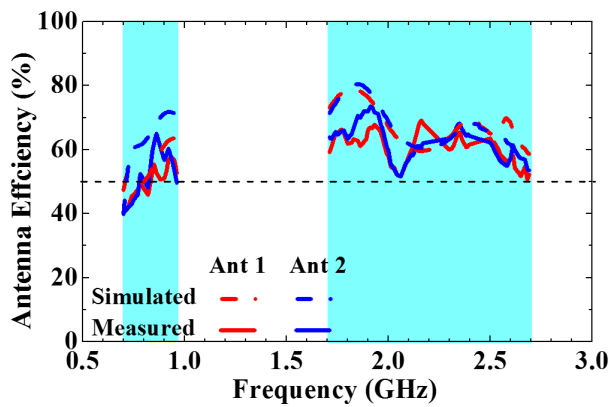


FIGURE 7. Measured and simulated antenna efficiencies for Ant 1 and Ant 2.

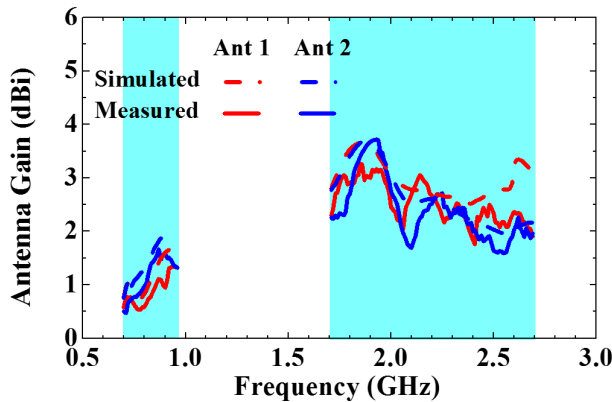


FIGURE 8. Measured and simulated antenna gains for Ant 1 and Ant 2.

Figure 7 exhibits the measured and simulated antenna efficiency obtained in the operating frequency bands of this LTE MIMO antenna system. There are slight difference between the measured antenna efficiencies of Ant1 and Ant2. It is probably owing to the tolerance associated with the lumped circuit elements and FR4 circuit board in the antenna fabrication. The measured efficiencies in the low- and high-frequency bands are about 40~65% and 51~73%, respectively, which are high enough for practical applications. Figure 8 shows the measured and simulated antenna

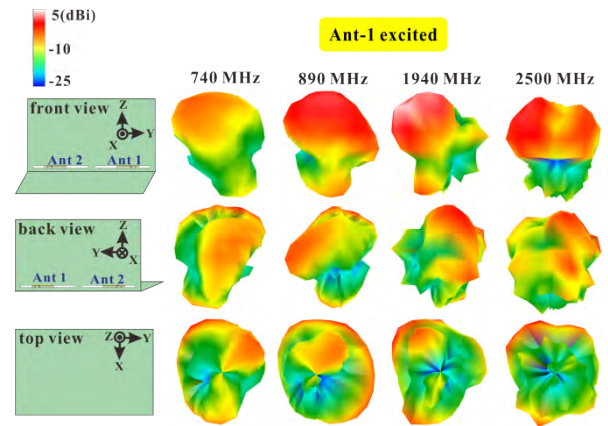


FIGURE 9. Measured 3D radiation patterns of Ant 1.

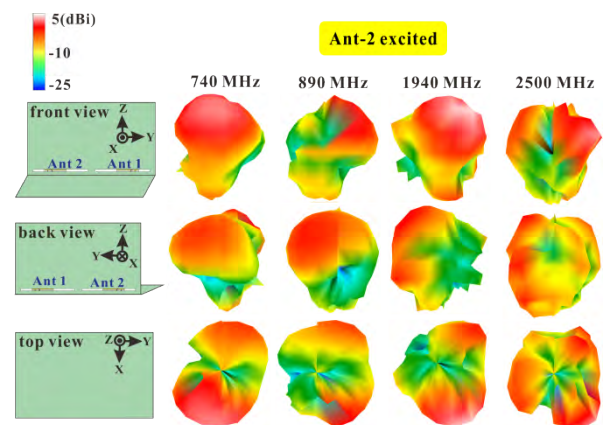


FIGURE 10. Measured 3D radiation patterns of Ant 2.

gains of the Ant1 and Ant2. The measured antenna gain is about 0.5~1.9 dBi in the low band, and 1.8~3.8 dBi in the high band.

Figures 9 and 10 are the measured 3D radiation patterns of Ant 1 and Ant 2 of the proposed MIMO antenna system, respectively, at four different frequencies, 740, 890, 1940, and 2500 MHz, which are around the center frequencies of the desired LTE700, GSM850/900, GSM1800/1900/UMTS, and LTE2300/2500 bands, respectively. It can be observed from the figures that the high-frequency radiation patterns have more depressions than the low-frequency ones because field distributions at high frequencies are more rapidly varied than at low frequencies. In addition, no matter which pattern is observed, the radiation in the +z direction is always stronger than that in the -z direction mainly because the keyboard ground plane acts partially as a reflector. Furthermore, the patterns in figures 9 and 10 exhibit mutual reflection symmetry with respect to the xz-plane, which is a reasonable result because Ant 1 and Ant 2 are structurally the mirror image of each other.

### C. MIMO ANTENNA SYSTEM CHARACTERISTICS ANALYSIS

Apart from the isolation between Ant 1 and Ant 2, the envelope correlation coefficient (ECC) between them is also

an important parameter to examine for a MIMO antenna system. In this study, the ECCs were calculated from the complex 3D electric-field patterns of Ant 1 and Ant 2 [22]. Figure 11 shows the measured and simulated ECCs of the proposed MIMO antenna system. As shown in the figure, the measured and simulated ECC values in the LTE frequency bands are all less than 0.2. Thus, it can be deduced that the two antennas of the proposed LTE MIMO antenna system have good channel independence.

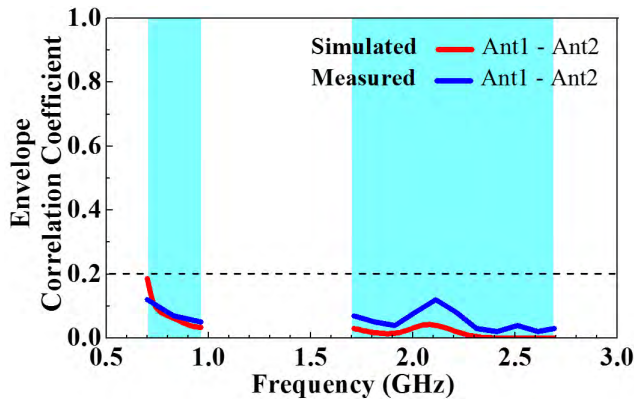


FIGURE 11. Measured and simulated ECCs of the proposed MIMO antenna system.

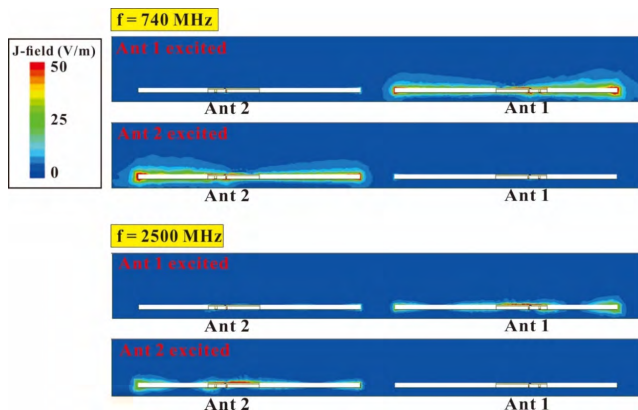


FIGURE 12. Surface current distributions on the ground plane at 740 and 2500 MHz when only Ant 1 or Ant 2 is excited.

To further understand the in-band interaction between Ant 1 and Ant 2 of the proposed LTE MIMO antenna system, we will study the ground-plane currents between the two antennas at 740 and 2500 MHz. Figure 12 shows these currents when only one of the two antennas is excited and the other is silent. When Ant 1 is excited, the ground-plane current circulates the closed slot of Ant 1, and no visible horizontal ground-plane flows to Ant 2. Similar phenomenon occurs when Ant 2 is excited. Therefore, it can be verified that the LTE MIMO antenna system has good isolation performance. It can be seen that the surface current distributions on the ground plane at 740 and 2500 MHz when only Ant 1 or Ant 2 is excited are  $1.0\lambda$  and  $2.0\lambda$  type are known as

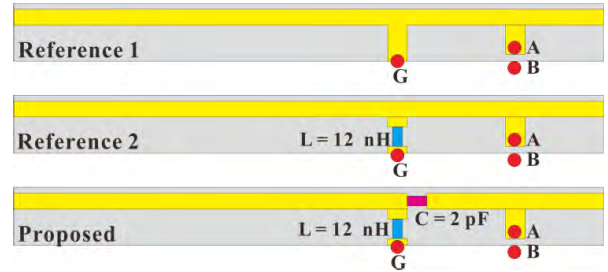


FIGURE 13. Reference 1, Reference 2, and proposed exciter structures.

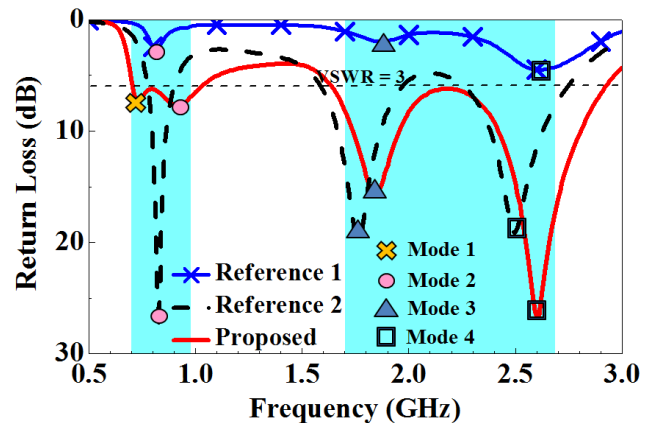


FIGURE 14. Simulated return loss of the closed slot antenna for three different exciters.

balanced types. Therefore, the proposed LTE MIMO antenna system has good isolation performance.

#### D. PARAMETRIC STUDIES

To better understand the design mechanism of the proposed LTE antenna, we will first carry out performance comparison for the antenna with three different exciters: the proposed, Reference 1, and Reference 2 exciters. The layout patterns of the three exciters are given in figure 13. For the Reference 1 exciter, no reactive chip elements are added in the PIFA structure. For the Reference 2 exciter, the chip inductor is embedded in the shoring segment. Figure 14 shows simulated return losses of the slot antenna for the three exciters. For the antenna with the Reference 1 exciter (no chip elements), only Modes 2, 3, and 4 of the closed slot structure are excited. They occur around 810, 1850, and 2630 MHz, the first one of which is within the desired low-frequency band and the last two of which are within the high-frequency band. However, the in-band impedance matching is very poor. When a 12 nH chip inductor is embedded in the shoring segment of the Reference 1 exciter to form the Reference 2 exciter, the impedance matching is greatly enhanced in both bands. However, Mode 1 is still not excited, the bandwidth associated with Mode 2 is not wide enough to cover the desired low-frequency band, and the return loss around 2100 MHz is still slightly smaller than 6 dB. Next, with an additional chip capacitor of 2 pF inserted in the

horizontal line segment of the Reference 2 exciter to form the proposed exciter, Mode 1 is finally excited and the impedance matching in the high-frequency band is further improved so that both the desired low- and high-frequency bands can be completely covered.

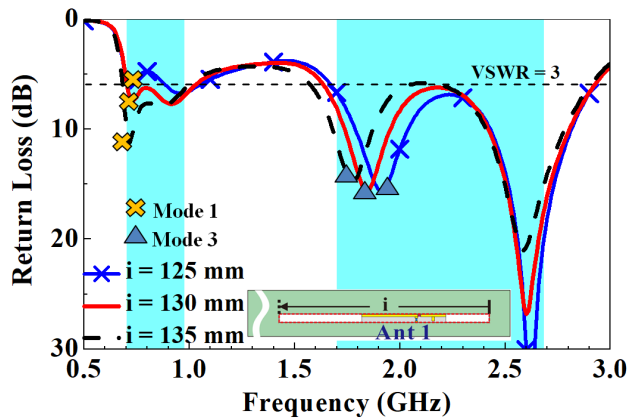


FIGURE 15. Simulated return loss for three different slot length parameters  $i$ .

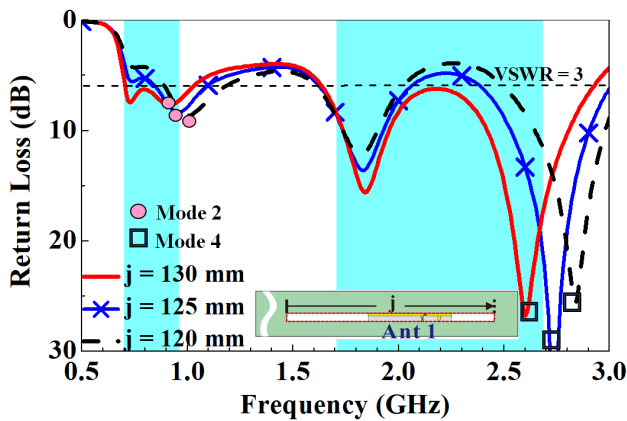


FIGURE 16. Simulated return loss for three different slot length parameters  $j$ .

To further explore the operating mechanism of this LTE antenna, we will study the effects of several relevant structural parameters on the antenna performance. Figure 15 shows simulated return losses of Ant 1 for three different slot lengths, denoted by  $i$ . Here, the portion of the closed slot to right of the exciter is fixed, and the left portion of the slot is varied. The considered slot lengths are 135, 130, and 125 mm. As can be seen from the comparison figure, when the length  $i$  is shortened from 135 to 125 mm, Mode 1 and Mode 3 tend to have higher resonant frequencies, thus verifying that Modes 1 and 3 are the modes contributed by the closed slot. On the contrary, if the left portion of the slot is fixed and the right portion is varied, the slot length for distinction purpose is denoted by  $j$ . The simulated return losses for  $j = 120, 125,$  and  $130$  mm are shown in figure 16, which indicates that when the slot is shortened from the

right end, Mode 2 and Mode 4 contributed by the closed slot tend to have higher resonant frequencies, thus verifying that Modes 2 and 4 are also the modes contributed by the closed slot. From the above results caused by the variations in the length parameters  $i$  and  $j$ , we have verified that Modes 1~4 are all the resonant modes contributed by the closed slot.

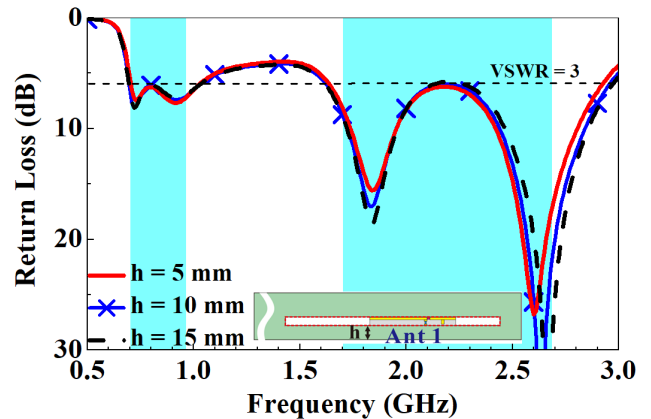


FIGURE 17. Simulated return loss of Ant 1 for three different parameters  $h$ .

Figure 17 presents simulated return losses of Ant 1 for three different separations, denoted by  $h$ , between the hinge and the lower edge of the closed slot. With  $h$  increases from 5 to 15 mm, its return loss does not change much, indicating that the antenna performance is not sensitive to this parameter. Nevertheless, the smallest one of  $h = 5$  mm among the three separations is chosen in the proposed design. The simulation done on the effect of the separation  $h$  can provide a reference for the practical configuration and application of the closed slot antenna.

Next, the change of the gap  $p$  between Ant 1 and Ant 2 is considered under the condition that the length of the closed slot and the relative location of the exciter in the closed slot are fixed. The increase of  $p$  leads to the decrease of the distance between Ant 1 (2) and the right (left) edge of the display ground plane. Figure 18 shows simulated  $S$ -parameters of the proposed MIMO antenna system for three different values of  $p$ . When  $p$  decreases from 25 to 15 mm, the reflection-coefficient curves remain almost unchanged, but the isolation ( $|S_{12}|$ ) decreases. The smallest isolation in the low band drops by about 2 dB, from 18 to 16 dB, and in the high band drops by about 3 dB, from 16 to 13 dB.

### III. PROPOSED MIMO ANTENNA SYSTEM COMPATIBILITY ANALYSIS

#### A. STUDY ON COMPATIBILITY OF INTEGRATION WITH PERIPHERAL METAL ELEMENTS

Besides the display and keyboard ground planes, some metal components may also exist in commercially available laptops. These metal components, such as a monitor to be integrated on the display ground plane and printed circuit boards and

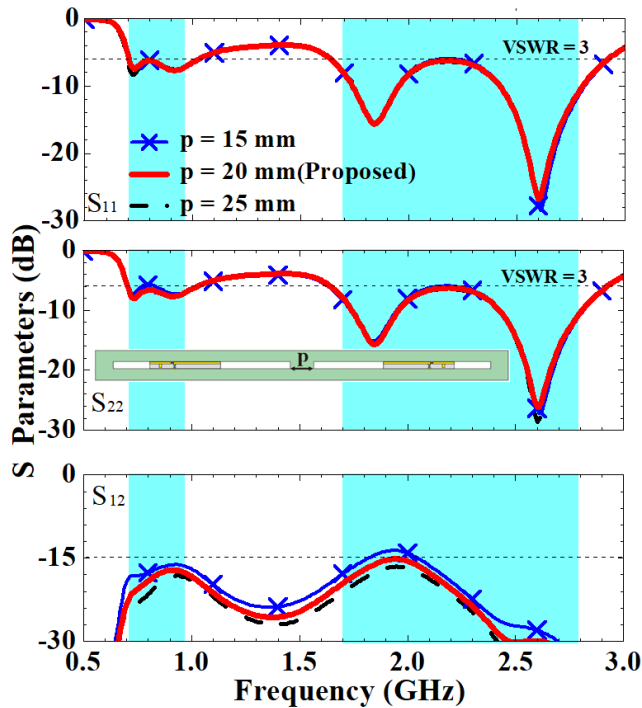


FIGURE 18. Simulated S-parameters of the MIMO antenna system for three different gaps between Ant 1 and Ant 2.

batteries to be integrated on the keyboard ground planes, may affect the performance of the MIMO antenna system to some degree. For the antenna system to be practical, its performance should not be severely downgraded by the presence of these metal components. Hence, it is worthwhile to check the compatibility of these metal components with the antenna system. Two cases are considered here: a metallic board of  $310 \times 180 \times 3 \text{ mm}^3$  on the display ground plane (denoted by board-1 in figure 19(a)) and a metallic board of the same size on the keyboard ground plane (denoted by board-2 in figure 19(b)). In figure 19(a), the lower edge of metallic board-1 aligns with the upper edge of the closed slots, and in figure 19(b), the metallic board-2 on the keyboard ground plane clings to the hinge.

Figure 20 shows simulated S-parameters of the proposed LTE MIMO antenna system with one of the two metallic boards integrated. For comparison, result of the proposed antenna system without an additional metallic board is also given in this figure. It can be seen that the isolation is not affected much by the added metallic boards. Although the impedance matching around 1.85 and 2.6 GHz deteriorates, the return loss stays above 6 dB in the whole high-frequency band in the presence of a metallic board. On the other hand, in the low-frequency band the smallest return loss occurring around 0.8 GHz reduces to below the criterion of 6 dB in the presence of metallic board-1. This is undesirable; yet, it is still larger than 5 dB, which is very close to the desired 6 dB. For mobile antennas deployed in a laptop, the efficiency is a very important parameter to examine to determine whether a design is acceptable or not. Figure 21 shows the

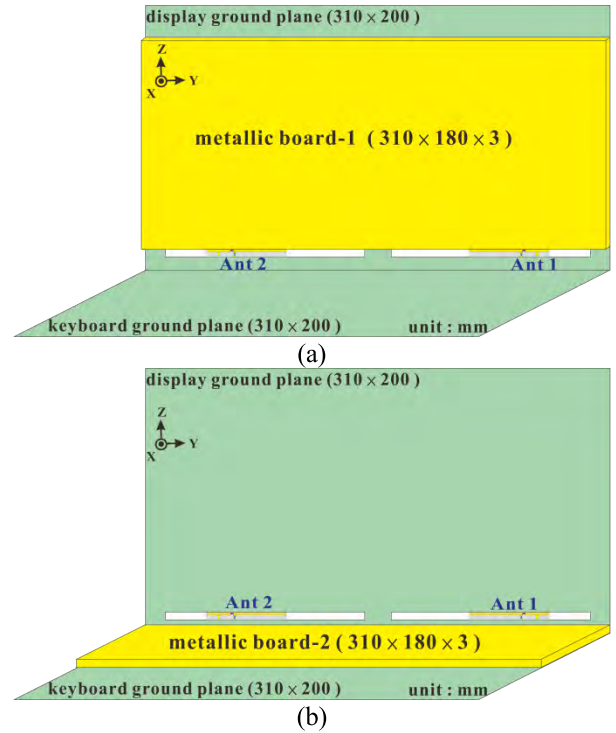


FIGURE 19. The structure of the proposed LTE MIMO antenna system integrated with a metallic board on the (a) display ground plane and (b) keyboard ground plane.

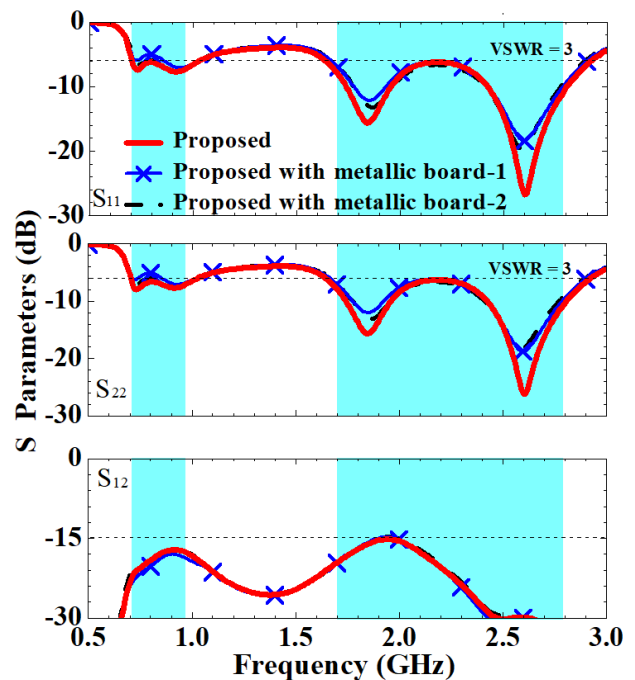


FIGURE 20. Simulated S-parameters of the proposed MIMO antenna system integrated with metallic boards.

corresponding simulated antenna efficiencies. Observe that in the high-frequency band the antenna efficiencies, greater than 65%, are not changed much when a metallic board is added to the proposed LTE MIMO antenna system. Around 0.8 GHz,

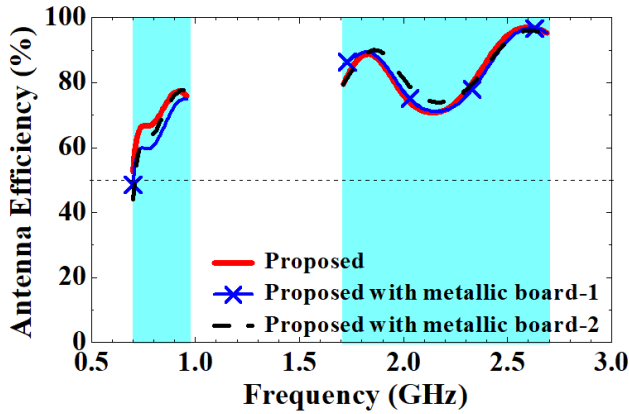


FIGURE 21. Simulated antenna efficiency of the proposed MIMO antenna system integrated with metallic boards.

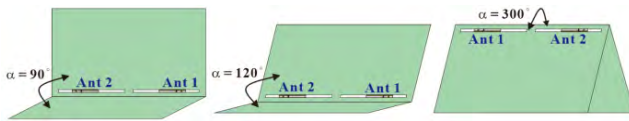


FIGURE 22. The LTE MIMO antenna system at three different laptop opening angles.

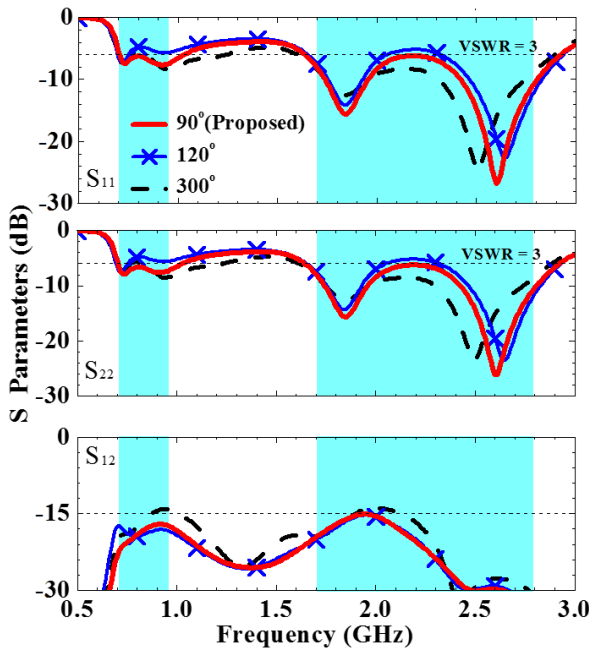


FIGURE 23. Simulated S-parameters of the proposed MIMO antenna system for three different opening angles of the laptop.

the frequencies where the return loss drops below 6 dB, the antenna efficiencies, whether with an additional metallic board or not, are still larger than 59%. The antenna efficiencies drop below 50% only around the lower edge frequencies of the low-frequency band. Nevertheless, the smallest one is still larger than 45%, which is acceptable for practical applications. In short, results shown in figures 20 and 21

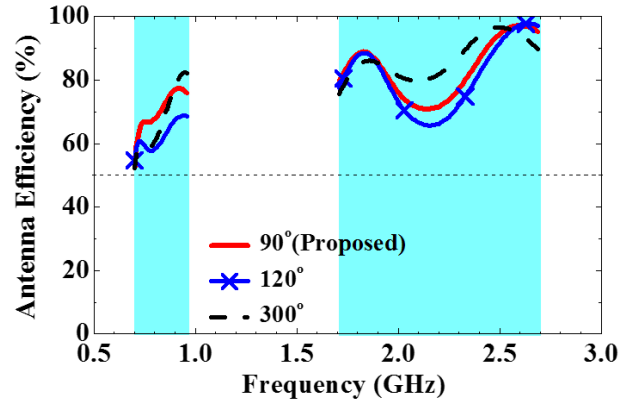


FIGURE 24. Simulated antenna efficiency of the proposed MIMO antenna system for three different opening angles of the laptop.

indicate that the proposed MIMO antenna system has very high integration compatibility.

**B. CHARACTERISTICS OF MIMO ANTENNA SYSTEM AT DIFFERENT LAPTOP OPENING ANGLES**

At present, many commercially available laptop computers can be used at different opening angles. In order to understand the practicality of this design, three commonly used opening angles of the laptop will be considered: 90° (the opening angle set in the design process), 120° (a very commonly used opening angle), and 300° (the opening angle frequently used in the multi-user sharing mode), as shown in figure 22. Figures 23 and 24 show simulated S-parameters and antenna efficiencies, respectively, of the proposed LTE MMO antenna system for these three laptop opening angles. As compared with the performance at the opening angle of 90°, the impedance matching at the opening angle of 300° deteriorates in most of the low-frequency band and in a small region of the high-frequency band, but with the return loss still greater than 5 dB. Fortunately, the corresponding simulated antenna efficiencies are still larger than 50%, implying that the proposed LTE MIMO antenna system still has good antenna performance under these three conditions.

**IV. CONCLUSION**

In this paper, a new LTE MIMO antenna system consisting of two mirror-imaged slot antennas have been designed and implemented on the display ground plane of a laptop computer. Each slot measures only 3 mm in width, and is excited by a PIFA structure with LC matching elements to support the operations of eight bands, i.e., LTE700/GSM850/900/1800/1900/UMTS/LTE2300/2500. With a small separation of 20 mm between the two slot antennas, the measured in-band isolation between them is already larger than 16 dB, even without adding any isolation element. The antennas efficiencies are larger than 40% and 50%, respectively, in both the low- and high-frequency bands. This antenna system is very suitable for implementation in laptop computers with a metal cover and a large screen-to-body ratio.



## REFERENCES

- [1] J.-H. Lu and F.-C. Tsai, "Planar internal LTE/WWAN monopole antenna for tablet computer application," *IEEE Trans. Antennas Propag.*, vol. 61, no. 8, pp. 4358–4363, Aug. 2013.
- [2] S.-C. Chen and K.-L. Wong, "Planar strip monopole with a chip-capacitor-loaded loop radiating feed for LTE/WWAN slim mobile phone application," *Microw. Opt. Technol. Lett.*, vol. 53, no. 4, pp. 952–958, Apr. 2011.
- [3] K.-L. Wong and P.-R. Wu, "Dual-wideband linear open slot antenna with two open ends for the LTE/WWAN smartphone," *Microw. Opt. Technol. Lett.*, vol. 57, no. 6, pp. 1269–1274, Jun. 2015.
- [4] C.-T. Lee, S.-W. Su, S.-C. Chen, and C.-S. Fu, "Low-cost, direct-fed slot antenna built in metal cover of notebook computer for 2.4-/5.2-/5.8-GHz WLAN operation," *IEEE Trans. Antennas Propag.*, vol. 65, no. 5, pp. 2677–2682, May 2017.
- [5] K.-L. Wong and T.-W. Weng, "Very-low-profile dual-wideband tablet device antenna for LTE/WWAN operation," *Microw. Opt. Technol. Lett.*, vol. 56, pp. 1938–1942, Aug. 2014.
- [6] K.-L. Wong and Z.-G. Liao, "Small-size dual-wideband monopole antenna with inductive and capacitive feeding branches for long term evolution tablet computer application," *Microw. Opt. Technol. Lett.*, vol. 57, no. 4, pp. 853–860, Apr. 2015.
- [7] K.-L. Wong and M.-T. Chen, "Very-low-profile dual-wideband loop antenna for LTE tablet computer," *Microw. Opt. Technol. Lett.*, vol. 57, no. 1, pp. 141–146, Jan. 2015.
- [8] K. L. Wong and Z. G. Liao, "Passive reconfigurable triple-wideband antenna for LTE tablet computer," *IEEE Trans. Antennas Propag.*, vol. 63, no. 3, pp. 901–908, Mar. 2015.
- [9] K.-L. Wong and C.-Y. Huang, "Triple-wideband open-slot antenna for the LTE metal-framed tablet device," *IEEE Trans. Antennas Propag.*, vol. 64, no. 12, pp. 5966–5971, Dec. 2015.
- [10] K.-L. Wong and Y.-J. Li, "Low-profile open-slot antenna with three branch slots for triple-wideband LTE operation in the metal-framed smartphone," *Microw. Opt. Technol. Lett.*, vol. 57, no. 10, pp. 2231–2238, Oct. 2015.
- [11] K.-L. Wong and C.-Y. Tsai, "Low-profile dual-wideband inverted-T open slot antenna for the LTE/WWAN tablet computer with a metallic frame," *IEEE Trans. Antennas Propag.*, vol. 63, no. 7, pp. 2879–2886, Jul. 2015.
- [12] K.-L. Wong and C.-Y. Tsai, "Dual-wideband U-shape open-slot antenna for the LTE metal-framed tablet computer," *Microw. Opt. Technol. Lett.*, vol. 57, no. 11, pp. 2677–2683, Nov. 2015.
- [13] Y. L. Ban, Y. F. Qiang, Z. Chen, K. Kang, and J. H. Guo, "A dual-loop antenna design for hepta-band WWAN/LTE metal-rimmed smartphone applications," *IEEE Trans. Antennas Propag.*, vol. 63, no. 1, pp. 48–58, Jan. 2015.
- [14] S.-C. Chen, C.-C. Huang, and W.-S. Cai, "Integration of a low-profile, long-term evolution/wireless wide area network monopole antenna into the metal frame of tablet computers," *IEEE Trans. Antennas Propag.*, vol. 65, no. 7, pp. 3726–3731, Jul. 2017.
- [15] S.-H. Chang and W.-J. Liao, "A compact 3D antenna with comprehensive LTE band coverage for use on notebook hinge," in *Proc. IEEE Asia-Pacific Conf. Antennas Propag.*, Singapore, Aug. 2012, pp. 142–143.
- [16] S.-C. Chen and Y.-C. Tsou, "Small-size LTE/WWAN two-strip monopole exciter antenna integration with metal covers," *IEEE Trans. Antennas Propag.*, vol. 64, no. 8, pp. 3707–3711, Aug. 2016.
- [17] W.-Y. Li, W.-J. Chen, and C.-Y. Wu, "Multiband 4-port MIMO antenna system for LTE700/2300/2500 operation in the laptop computer," in *Proc. APMC*, Kaohsiung, Taiwan, Dec. 2012, pp. 1163–1165.
- [18] S. C. Chen, P. W. Wu, C.-I. G. Hsu, and J. Y. Sze, "Integrated MIMO slot antenna on laptop computer for eight-band LTE/WWAN operation," *IEEE Trans. Antennas Propag.*, vol. 66, no. 1, pp. 105–114, Jan. 2018.
- [19] S. Cheng, P. Lindberg, A. Kaikkonen, and P. Hallbjörner, "Internal multiple-input, multiple-output antenna arrays for wireless wide area network and wireless local area network operation in seamless full metal cover laptops," *IET Microw., Antennas Propag.*, vol. 8, no. 2, pp. 73–79 2014.
- [20] S.-C. Chen and C.-S. Fu, "Switchable long-term evolution/ wireless wide area network/ wireless local area network multiple-input and multiple-output antenna system for laptop computers," *IEEE Access*, vol. 5, pp. 9857–9865, May 2017.
- [21] *Corporation HFSS*. Accessed: Jun. 14, 2018. [Online]. Available: <http://www.ansys.com/products/electronics/ansys-hfss>
- [22] M. P. Karaboikis, V. C. Papamichael, G. F. Tsachtsiris, C. F. Soras, and V. T. Makios, "Integrating compact printed antennas onto small diversity/MIMO terminals," *IEEE Trans. Antennas Propag.*, vol. 56, no. 7, pp. 2067–2078, Jul. 2008.



**SHU-CHUAN CHEN** (M'13) received the B.S. and M.S. degrees in electrical engineering from the Chung Cheng Institute of Technology (CCIT), National Defense University (NDU), Taoyuan, Taiwan, in 1998 and 2004, respectively, and the Ph.D. degree in electrical engineering from National Sun Yat-sen University, Kaohsiung, Taiwan, in 2012. Since 2012, she has been an Assistant Professor with the Department of Electrical and Electronic Engineering, CCIT, NDU, where she became an Associate Professor, in 2016. She holds over 20 patents, including USA, Taiwan, and Chinese patents. Her current research interest includes internal antennas for mobile communication devices.



**MING-CHAN HSU** received the B.S. degree from Feng Chia University, Taichung, Taiwan, in 2014, and the M.S. degree from the National Yunlin University of Science and Technology, Douliu, Taiwan, in 2017, both in communications engineering. His current research interests include antenna and microwave circuit design.

...